

# Miniaturized Spiral Planar Inverted F Antenna of 2.4 GHz Using Design of Experiment Method for EEG-based Controlled Prosthetic Arm

Liya Yusrina Sabila<sup>a,\*</sup>, Teguh Prakoso<sup>b</sup>, Munawar Agus Riyadi<sup>b</sup>

<sup>a</sup>Department of Electrical Engineering  
University of Ahmad Dahlan

Jl. Ringroad Selatan, Kragilan, Tamanan, Kec. Banguntapan, Bantul  
Yogyakarta, Indonesia

<sup>b</sup>Department of Electrical Engineering  
University of Diponegoro

Jl. Prof. Sudarto No.13, Tembalang, Kec. Tembalang  
Semarang, Indonesia

## Abstract

This paper presents the design of a planar inverted F antenna with a miniature or tiny shape at the frequency of 2.4 GHz. The antenna uses a spiral design to reduce the dimension of the antenna with conformal shape for a suitable prosthetic arm. Usually, the antenna design uses long experimental steps, namely trial and error. It can be summarized using the DOE (design of experiment) method. The DOE is a method to streamline the experimental steps to get the best design. The DOE method uses a tuning reference at the design parameter variation of  $\pm 5\%$  of the nominal value. Four tuning steps can get the best results from  $S_{11}$ , bandwidth, and gain. The designed antenna works at the resonant frequency of 2.431 GHz with the value of  $S_{11}$  is -22.634 dB, bandwidth of 37.1 MHz, and gain of -7.596 dBi.

**Keywords:** antenna, PIFA, spiral design, 2.4 GHz, conformal antenna, prosthetic arm.

## I. INTRODUCTION

A prosthetic device plays important role in helping disabled people improve their ability to manage daily activities and stay independent. A prosthetic arm is one among a wide variety of prosthetic devices. Previous studies in [1]-[2] discussed the use of EEG (electroencephalogram) signals for brain-computer interface (BCI) applications, particularly for controlling a prosthetic arm. The communication between the brain and the arm is established by collecting EEG signals captured from the scalp using electrodes. To transmit EEG signals, wireless communications have grown in popularity compared to wired communication due to its compact size and the flexibility in supporting the movement. Antenna module is an important element in wireless system to convert electric current into electromagnetic radiation and vice versa [3]-[4]. The frequency used for this transmission is 2.4 GHz. This antenna enables short-distance data transmission between the EEG and prosthetic arm and typically uses Bluetooth and WiFi technology [5]-[7].

In antenna design, antenna size is one of the design problems. Large antennas are certainly challenging to be applied to other devices. Therefore, the proposed antenna offers a miniature antenna using a spiral shape while

maintaining good performance. A spiral shape is known to reduce the dimensions of the antenna [8]-[11]. In addition to having a small shape, the antenna design challenges adjusting the shape to the prosthetic arm's curve. So, it is necessary to apply a conformal technique. The conformal technique makes the antenna have a curved shape that can follow the shape of the prosthetic arm [12]-[13]. Having a miniature and conformal shape will make it easier to place the antenna on the prosthetic arm.

In this study, the DOE (design of experiment) method was used to avoid the trial-and-error method, where it is unknown how many experimental steps must be passed. The DOE method can summarize the steps in designing an antenna to get the best results. The size of the change in each parameter presented is also obtained from the calculation, so the size used is not approximate. The DOE method has been applied in filter design [14], demonstrates the certainty of shift changes, and simplifies design steps. The research method of antennas is explained in Section 2, whereas Section 3 presents results and discussion, and Section 4 is the conclusion.

## II. METHOD

In designing an antenna using DOE, several steps need to be done. It can be shown in Figure 1.

### A. Spiral Planar Inverted F Antenna (PIFA)

Planar inverted F antenna (PIFA) is a very popular design in mobile communication. The design of PIFA is shown in Figure 2 [15]. The resonant frequency of the PIFA antenna is determined by the length of patch  $L$ , the

\* Corresponding Author.

Email: liya.sabila@te.uad.ac.id

Received: October 27, 2021 ; Revised: January 24, 2022

Accepted: March 8, 2022 ; Published: August 31, 2022

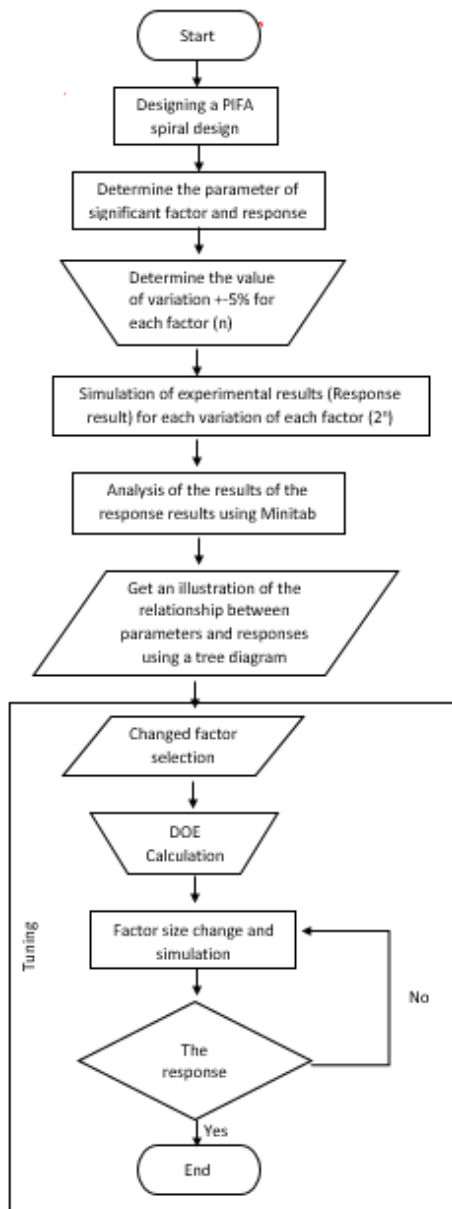


Figure 1. Step in designing an antenna using DOE

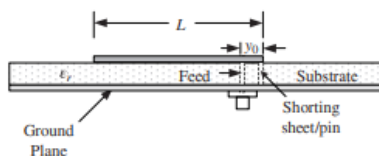


Figure 2. Planar inverted-F antenna (PIFA) design

width of patch  $W$ , the width of the short circuit film  $w_s$ , and the height of the substrate  $h$ . As a general rule, the height  $h$  is small and can be ignored. When ignoring height, the main design limitation is the  $1/4$  wavelength spacing between the pin and the opposite edge of the patch. Therefore, if the short-circuit sheet extends across the width of the patch, the distance  $L$  is equal to  $1/4$  wavelength. In summary, the design equation can be seen in (1)

$$L + W - w_s = \frac{\lambda}{4} + h \quad (1)$$

The spiral design is a series of horizontal and vertical lines. The spiral line can be used as a typical antenna element to reduce its size due to its slow wave (SW) structure.

These wired SW structures are advantageous in designing a small antenna because a self-resonance condition is easily attained, even though the antenna dimensions are small. In small antennas, self-resonance is significant because it helps mitigate the matching difficulty in a small antenna arising from its impedance, which is a very low and large resistive component that may combine to produce a large loss and degrade the antenna performance. The wired SW structures have additional advantages: simple fabrication, low cost, and can be constructed in planar form, which is very useful for small equipment such as small handsets, handy mobile terminals, and so forth [16].

## B. Specifications and Initial Design

Before starting the design, the antenna specifications have been developed, as seen in Table 1. The antenna design was simulated using CST Microwave Studio, and the DOE analysis was performed using Minitab 7. This antenna uses FR dielectric material with a dielectric constant of 4.3, the board thickness is 1.6 mm, and the thickness of the conductive material (copper) is 0.035 mm. The nominal size of the PIFA was calculated directly from its design formulas in Table 2. The initial design of the faces top and side is shown in Figures 3 and 4.

The  $S_{11}$  result of the initial antenna design is shown in Figure 5. We can see that the result of  $S_{11}$  does not meet specifications. A 2.314 GHz is the resonant frequency, and the bandwidth is 20.4 MHz. It is necessary to agree with the analysis of the DOE method to obtain the best  $S_{11}$  value, the resonant frequency, and the bandwidth.

TABLE 1  
SPECIFICATIONS ANTENNA

Parameter	Specification
Frequency range	2.4 GHz – 2.484 GHz
Resonant frequency	2.422 GHz
Bandwidth	84 MHz
$S_{11}$	$\leq -10$ dB
Gain	$\geq -10$ dBi
Radiation pattern	Omnidirectional

TABLE 2  
NOMINAL SIZE OF PIFA SPIRAL

Factor	Size
Line width ( $W_p$ )	1 mm
Radius shorting pin ( $P_1$ )	0.6 mm
Radius feed ( $P_2$ )	0.4 mm
Short and feed distance ( $G_x$ )	4 mm
Line length 1 ( $L_{p1}$ )	2.5 mm
Line length 2 ( $L_{p2}$ )	7 mm
Gap ( $S$ )	1 mm
Length substrate ( $L_s$ )	12 mm
Width substrate ( $W_s$ )	8 mm

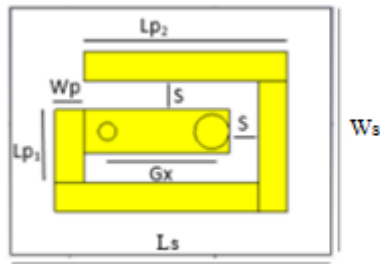


Figure 3. Spiral PIFA design (top view)

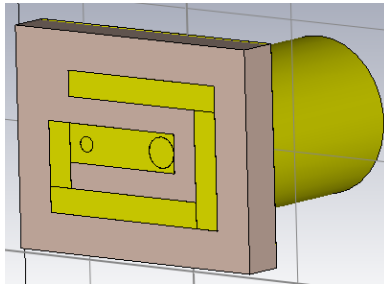
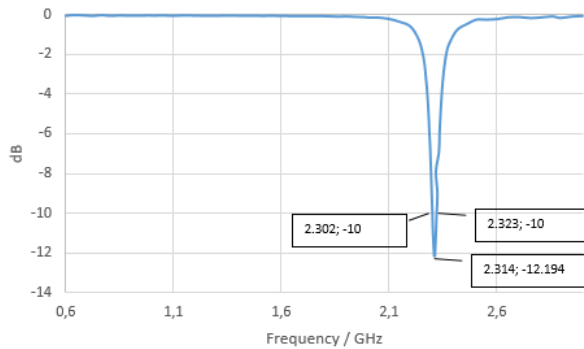


Figure 4. Spiral PIFA design (side view)


 Figure 5.  $S_{11}$  result of the initial spiral PIFA design

### C. Effect of Conformal Shape and Prosthetic Arm Material

A conformal shape is introduced to correct the curved shape of the antenna. The size of diameter of the antenna arch is 7 cm, following the diameter in the human elbow area. An antenna with a conformal shape is shown in Figure 6, and the addition of prosthetic arm material and silicone is shown in Figure 7.

Following the conformal shape and adding a material prosthetic arm to PIFA can change the antenna's performance. As shown in Table 3, there is a shift from the resonant frequency to a higher frequency of 7 MHz for the conformal shape from the flat shape and a shift to a lower frequency to 6 MHz for the addition of material prosthetic arm from the conformal shape. The bandwidth is reduced in conformal shape to 11 MHz and 0.3 MHz on prosthetic arm material. Meanwhile, adding a prosthetic arm material gives the  $S_{11}$  a better result than a flat antenna.

### D. Design of Experiment

From the resonant frequency results in Table 3, the results are not close to specifications. In this case, tuning

 TABLE 3  
COMPARISON OF PIFA SPIRAL PERFORMANCE

Spec.	Flat Shape	Conformal Shape	Prosthetic Arm
Frequency range	2.302 – 2.323 GHz	2.315 – 2.325 GHz	2.264 – 2.284 GHz
Resonant frequency	2.314 GHz	2.321 GHz	2.275 GHz
Bandwidth	20.4 MHz	9.4 MHz	20.1 MHz
$S_{11}$ (dB)	-12.194 dB	-10.431 dB	-12.212 dB
Gain (dBi)	-16.503 dBi	-14.891 dBi	-12.497 dBi
Radiation Pattern	Omnidirectional	Omnidirectional	Omnidirectional

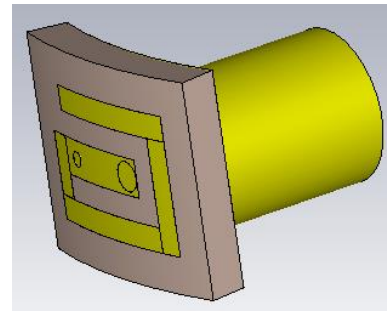


Figure 6. Conformal antenna design

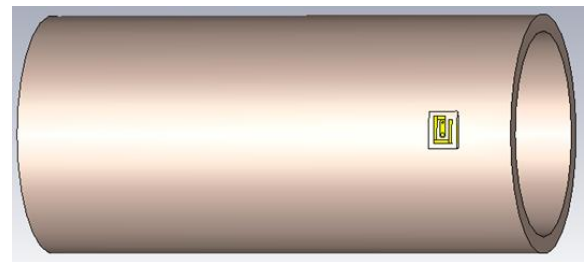


Figure 7. Antenna with prosthetic arm material

is needed to shift low resonant frequency into high resonant frequency. Before tuning, the DOE method analyzes the relationship between the selected antenna parameters that affect the desired response. From Table 4, four important factors are chosen. These are  $L_{p1}$ ,  $L_{p2}$ ,  $S$ , and  $W_p$ . While  $S_{11}$ , the resonant frequency, and bandwidth are response values.

The values in Table 4 represent  $\pm 5\%$  of the nominal value. Label (-1) means a -5% change, and label (+1) represents a +5% change from the nominal value in Table 2. From four factors, there are 16 experiments ( $2^4$ ) with the response of  $S_{11}$ , the resonant frequency, and the bandwidth, as shown in Table 5. In analyzing the DOE method, Minitab software illustrates the relationship between factors and responses using a tree diagram, as shown in Figure 8. The tree diagram provides the factor's

 TABLE 4  
VARIATION VALUE IS  $\pm 5\%$  FOR 2 VARIABLES

Factor	-1	+1
$L_{p1}$	2.375	2.625
$L_{p2}$	6.65	7.35
$S$	0.95	1.05
$W_p$	0.95	1.05

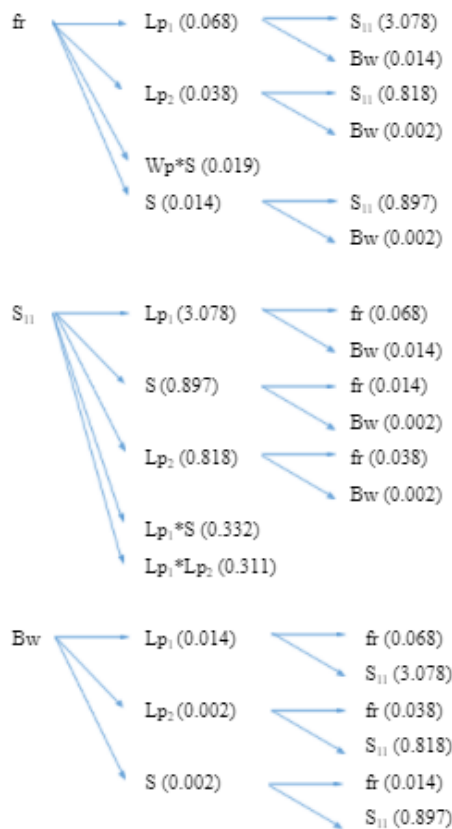


Figure 8. Tree diagram of the relationship between parameter factors to the response

TABLE 5  
RESPONSE RESULT OF 4 FACTORS

No.	Factors				Responses		
	Wp	Lp <sub>1</sub>	S	Lp <sub>2</sub>	S <sub>11</sub> (dB)	<i>f<sub>r</sub></i> (GHz)	bw (GHz)
1.	-1	-1	-1	-1	-14.780	2.386	0.028
2.	-1	-1	-1	1	-12.834	2.304	0.023
3.	-1	-1	1	-1	-17.406	2.374	0.033
4.	-1	-1	1	1	-14.976	2.297	0.027
5.	-1	1	-1	-1	-8.657	2.239	0
6.	-1	1	-1	1	-7.763	2.167	0
7.	-1	1	1	-1	-9.9	2.232	0
8.	-1	1	1	1	-8.927	2.16	0
9.	1	-1	-1	-1	-14.948	2.347	0.029
10.	1	-1	-1	1	-13.133	2.268	0.023
11.	1	-1	1	-1	-17.995	2.414	0.034
12.	1	-1	1	1	-15.151	2.338	0.027
13.	1	1	-1	-1	-9.18	2.213	0
14.	1	1	-1	1	-8.128	2.141	0
15.	1	1	1	-1	-10.28	2.275	0.007
16.	1	1	1	1	-9.141	2.206	0

sensitivity (slope) value to the response. To obtain optimal results on the design of PIFA, three adjustments are required, as shown in Table 6.

### III. RESULT AND DISCUSSION

This section discusses the tuning process's steps, the research results, and a comparison between flat,

TABLE 6  
TUNING PROCESS

Factor	Nominal	Tuning 1	Tuning 2	Tuning 3	Tuning 4
Lp <sub>1</sub>	2.5	2.317	2.317	2.317	2.317
Lp <sub>2</sub>	7	7	6.647	6.647	6.647
S	1	1	1	1.117	1.13
Wp	1	1	1	1	1

conformal, and antenna with prosthetic arm material (with some tuning).

#### A. Tuning 1

Tuning 1 is done to increase bandwidth. The bandwidth at the center frequency increased to 40 MHz, from the initial 20.1 MHz. Then obtained an increase of  $40 - 20.1 = 19.9$  MHz. According to the tree diagram in Figure 5, the most significant factor in increasing the bandwidth is Lp<sub>1</sub>, with a coefficient of 0.014 for each +5 % change of the nominal length. For the bandwidth to increase to 40 MHz, Lp<sub>1</sub> must be changed by  $(0.02)/0.014 = 1.465$  or 73.27 %. If 73.27 % of 2.5 mm is 0.183 mm. Then Lp<sub>1</sub> becomes 2.317 mm. Tuning one increases the bandwidth to 29.8 MHz with a value of S<sub>11</sub> -16 dB and a resonant frequency of 2.335 GHz.

#### B. Tuning 2

In tuning 2, it is done to shift the resonant frequency by changing the Lp<sub>2</sub> factor. The resonant frequency of 2.335 GHz will be shifted to 2.442 GHz. Then obtained a shift of  $2.442 - 2.335 = 0.107$  GHz. The slope used in tuning 2 is the coefficient of Lp<sub>1</sub> and Lp<sub>2</sub>, which is 0.106. For the resonant frequency to shift to 2.442 GHz, Lp<sub>2</sub> must be changed by  $(0.107)/0.106 = 1.009$  or equivalent to 5.043 %. If 5.043 % of 7 mm is 0.353 mm. Then Lp<sub>2</sub> becomes 6.647 mm, and the impact of the frequency shift to 2.374 GHz with an S<sub>11</sub> value of -17.3 dB.

#### C. Tuning 3

The value of S<sub>11</sub> (*f<sub>r</sub>*) of -17.3 dB will be reduced to -30 dB. Then it is obtained, the change in S<sub>11</sub>  $-30 - (-17.3) = -12.7$  dB. In tuning 3, S changes with a coefficient of 0.897 for each +5 % change of the nominal length. However, in the 1st and 2nd tuning, changes have been made to Lp<sub>1</sub> and Lp<sub>2</sub>, so the coefficients used in this case are Lp<sub>1</sub>, S, Lp<sub>2</sub>, Lp<sub>1</sub>\*S, and Lp<sub>1</sub>\*Lp<sub>2</sub>, becoming 5.437. For the value of S<sub>11</sub> to be -30 dB, S must be changed by  $(12.7)/5.437 = 2.329$  or equivalent to 11.646 %. If 11.646 % of 1 mm is 0.117 mm. Then S becomes 1.117 mm, and the impact of changing the value of S<sub>11</sub> to -25.9 dB with *f<sub>r</sub>* of 2.472 GHz.

#### D. Tuning 4

The center frequency on S<sub>11</sub> (*f<sub>r</sub>*) of 2.472 GHz will be shifted to 2.442 GHz. Get a shift of  $2.472 - 2.442 = 0.03$  GHz. In tuning 4, the S changes again. Tuning 4 using the same coefficients Lp<sub>1</sub>, Lp<sub>2</sub> and S become 0.12. For *f<sub>r</sub>* to shift to 2.442 GHz, S must be changed by  $(0.03)/(0.12) = 0.249$  or the equivalent of 1.013 %. If 1.013 % of 1.117 is 0.014 mm. S becomes 1.13 mm and has the effect of shifting *f<sub>r</sub>* to 2.412 GHz, has a value of S<sub>11</sub> -22.6 dB, and bandwidth of 37.1 MHz.

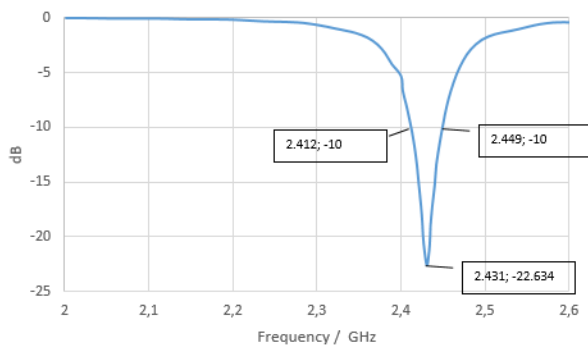

 Figure 9. The final result of  $S_{11}$ 

Figure 9 shows the final result of  $S_{11}$ . In this variable,  $W_p$  does not change because in tuning 4, the performance results shown are maximum, and tuning stops at tuning 4. The resulting frequency range is 2.412 – 2.429 GHz, and  $S_{11}$  is -22.634 dB. This performance result is the most optimal. In this case, the bandwidth does not meet the specifications. The next tuning was tried to obtain bandwidth but was not found. This is because of other changes in response, such as the shift in the resonant frequency value when the bandwidth is widened. Then the solution is to stop the tuning on the 4<sup>th</sup> tuning.

In each tuning, the changed parameters may not only shift the selected result. But it can also shift other results. For example, in tuning 1,  $L_{p1}$  is used to increase the bandwidth. However, in Figure 8,  $L_{p1}$  affects not only the shift in bandwidth but also the shift in the resonant frequency and the value of  $S_{11}$ . In this case, selecting the tuning process parameters should be taken.

### E. Gain and Radiation Pattern

The gain of the antenna designed based on the simulation is shown in Figure 10, with a value of -7.596 dBi. The radiation pattern is shown from the elevation radiation pattern in Figure 11 and the azimuth radiation pattern in Figure 12. Both radiation patterns indicate that the radiation pattern is omnidirectional.

The blue, green, and red colors in Figure 10 are the axes related to the radiation pattern in Figures 11 and 12. If we want to see the elevation radiation pattern, we can use a red line or the phi axis with a value of 0 degrees or the same as Figure 10 sliced horizontally. Conversely, if we want to see the azimuth radiation pattern, we can use

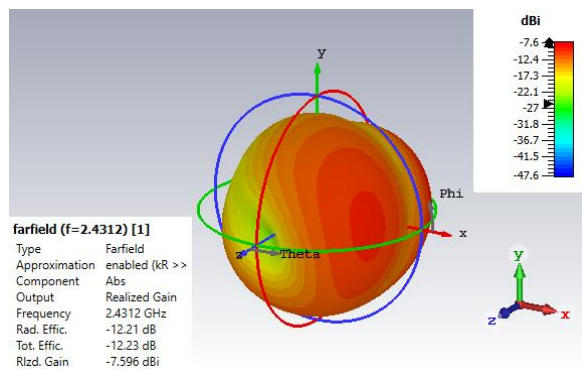


Figure 10. Gain simulation result

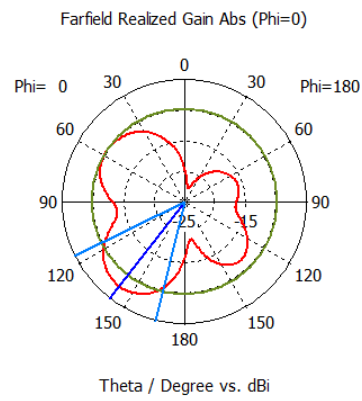


Figure 11. Elevation radiation pattern

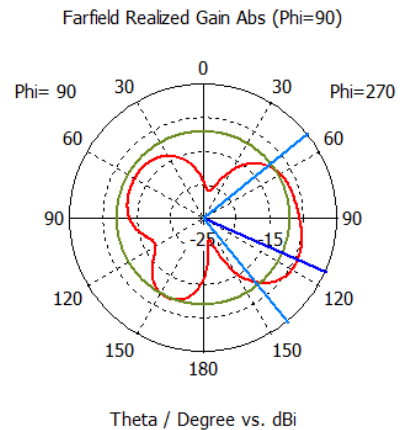


Figure 12. Azimuth radiation pattern

the red line or the phi axis with a value of 90 degrees or the same as Figure 10 sliced vertically.

### F. Comparison of DOE Method with Another Optimization

The DOE method makes it easy to determine how much change is needed in each selected parameter to achieve the goal. In section 4, it is shown that only four times the size changes on certain parameters can get the best results when compared with another optimization like on paper in [17]. In this study, the authors present many steps that need to be taken in changing one parameter. For example, in changing  $L_{p1}$ , the author conducted several experiments with a 0 – 8 mm size. Likewise, for changes to the  $L_{p2}$  parameter. Then the new size is chosen which is the most appropriate. This step is inefficient because it takes a long time to get all the data according to the specified range without any reference. Therefore, it is concluded that the DOE method provides an advantage for the antenna designer in changing the parameters according to the expected response.

### G. Measurement

Measurement of  $S_{11}$  on the antenna was done using Vector Network Analyzer SAA-2. The fabricated antenna can be seen in Figure 13. If the antenna is placed next to a 100-rupiah coin, the size of the antenna looks smaller or equal to the size of the coin. Based on the simulation results using CST Microwave Studio 2019,  $S_{11}$  measurements, and the SAA-2 Network Analyzer, an



Figure 13. Fabricated antenna

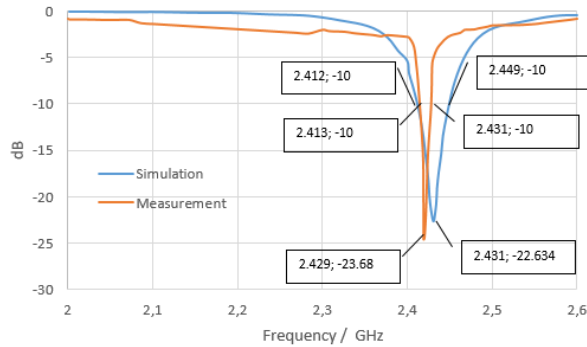
Figure 14. The comparison of the  $S_{11}$  antenna between simulation and measurement results

TABLE 7  
COMPARISON OF MEASUREMENT AND SIMULATION AT THE RESONANT FREQUENCY AND  $S_{11}$

	$S_{11}$ (dB)	Frequency (GHz)
Simulation	-22.634	2.431
Measurement	-23.681	2.429

image is obtained in the form of a comparison graph of the frequency relationship with the  $S_{11}$  results obtained in decibels (dB) between the simulation results and the size as shown in Figure 14. The horizontal axis shows the frequency range of 2 – 2.6 GHz, and the vertical axis shows the value of  $S_{11}$  in dB.

There is a shift in the resonant frequency and the value of  $S_{11}$  between the simulation and measurements on the antenna, as shown in Table 7. The shift in the resonant frequencies and the difference in the value of  $S_{11}$  between the simulation results and measurements on the designed PIFA meander is probably due to an inaccuracy in the size of the antenna during fabrication.

A frequency shift of 2 MHz, for example, can be caused by changes in the  $L_{p1}$  size during fabrication. According to the calculation, the result of dividing the difference between the measurement and simulation resonance frequencies is divided by the slope of  $L_{p1}$ ,  $\frac{0.002}{0.068} = 0.029$  and equivalent to 0.1471 %. If 0.1471 % of 2.317 mm is 0.003 mm. Then the size of  $L_{p1}$  becomes 2.32 mm.

#### IV. CONCLUSION

From the research, it has been proven that using the DOE method can make it easier. Just need four tuning processes can successfully obtain the best performance. The tuning process with the design-of-experiment method has been shown to shift the center frequency around 150 MHz and increase the bandwidth to about 20

MHz. The  $S_{11}$  presented result shows an effect that occurs due to the addition of prosthetic material (silicone) or from the conformal technique. The final result shows that values of  $S_{11}$ , resonant frequency, gain, and radiation pattern met specifications. The final design has a resonant frequency of 2.431 GHz with  $S_{11}$  of -22.634 dB, bandwidth of 37.1 MHz, and gain of -7.594 dBi. From this research, it can be said that the designed antenna is suitable to be proposed for a prosthetic arm. In fabrication, conformal forms can be realized using a 3D printer. However, this study also has alternative suggestions. Because the antenna size is tiny, the antenna can be fabricated by implementing the antenna into the prosthetic arm without bending the antenna.

#### DECLARATIONS

##### Conflict of Interest

The authors have declared that no competing interests exist.

##### CRedit Authorship Contribution

Liya Yusrina Sabila: Methodology, Software, Validation; Teguh Prakoso: Conceptualization, Funding Acquisition; Munawar Agus Riyadi: Supervision, Writing – Review & Editing.

##### Funding

Research reported in this publication was supported by Faculty of Engineering Universitas Diponegoro under grant number 05/UN7.P/KP/2019.

##### Acknowledgment

The authors thank the Faculty of Engineering Universitas Diponegoro for the financial support under Faculty's 4 Strategic Research Grant 2021.

#### REFERENCES

- [1] O. Chinbat and J. S. Lin, "Prosthetic arm control by human brain," in *Proc. 2018 Int. Symp. Comput. Consum. Control*, 2018, pp. 54–57, doi: 10.1109/IS3C.2018.00022.
- [2] M. A. Riyadi, T. Prakoso, F. O. Whaillan, M. David Wahono, and A. Hidayatno, "Classification of EEG-based brain waves for motor imagery using support vector machine," in *Proc. 2019 3rd Int. Conf. Electr. Eng. Comput. Sci.*, 2019, pp. 422–425, doi: 10.1109/ICECOS47637.2019.8984565.
- [3] R. Kaur, Surekha, and N. Kumar, "Study of planar inverted-F antenna (PIFA) for fourth generation wireless devices," *Int. J. Mod. Comput. Sci.*, vol. 4, no. 2, pp. 35–37, 2016.
- [4] Anjali and A. Kaur, "Performance analysis of patch and PIFA antenna for WCS and SDR applications," *Int. J. Adv. Res. Comput. Commun. Eng.*, vol. 6, no. 7, pp. 265–269, Jul. 2017.
- [5] S. Kumar, and M. Singh, "Big data analytics for healthcare industry: Impact, applications, and tools," *Big Data Mining Anal.*, vol. 2, no. 1, pp. 48–57, Mar. 2019, doi: 10.26599/BDMA.2018.9020031.
- [6] L. M. Ang, K. P. Seng, G. K. Ijamaru, and A. M. Zungeru, "Deployment of IoV for smart cities: Applications, architecture, and challenges," *IEEE Access*, vol. 7, pp. 6473–6492, 2019, doi: 10.1109/ACCESS.2018.2887076.
- [7] B. P. L. Lau *et al.*, "A survey of data fusion in smart city applications," *Inf. Fusion*, vol. 52, pp. 357–374, Dec. 2019, doi: 10.1016/j.inffus.2019.05.004.
- [8] A. Munir, A. Harish, and Chairunnisa, "Size reduction of UHF planar inverted-F antenna with patch geometry modification," in *2014 Int. Symp. Antennas Propag. Conf. Proc.*, pp. 537–538, 2014, doi: 10.1109/ISANP.2014.7026763.
- [9] R. Kumar, L. S. Solanki, and S. Singh, "Miniature archimedean spiral PIFA antennas for biomedical implantable devices," in

- 2019 6th Int. Conf. Signal Process. Integr. Netw., pp. 162–167, 2019, doi: 10.1109/SPIN.2019.8711600.
- [10] A. Harish, and A. Munir, "Compact circularly spiral planar inverted-F antenna for medical implant application," in *Proc. Int. Conf. Elect. Eng. Comput. Sci. Inform.*, pp. 488–491, 2014.
- [11] P. Soontornpipit, "Design and development of a dual-band PIFA antenna for brain interface applications," in *2019 7th Int. Elect. Eng. Congr.*, 2019, doi: 10.1109/ieecon45304.2019.8939014.
- [12] S. Sayah and R. Sarkis, "Design and analysis of conformal antennas for smart watch," in *Proc. 2017 Prog. Electromagn. Res. Symp. Fall*, 2017, pp. 1889–1894, doi: 10.1109/PIERS-FALL.2017.8293446.
- [13] R. Zabih and R. G. Vaughan, "Conformal axial-direction PIFA on a small cylinder," in *Proc. 2017 XXXII Ind General Assem. Scientific Symp. Int. Union Radio Science*, 2017, doi: 10.23919/URSIGASS.2017.8105234.
- [14] T. Prakoso, I. A. Utami, I. Santoso, M. A. Riyadi, and M. Facta, "Systematic tuning of coupled-line filter using DOE method," in *Proc. 2018 3rd Int. Conf. Inf. Technol. Inf. Syst. Electr. Eng.*, pp. 391–395, 2018, doi: 10.1109/ICITISEE.2018.8720981.
- [15] C. A. Balanis, *Antenna Theory: Analysis and Design*, 4th ed. Hoboken, New Jersey: John Wiley & Sons, Inc., 2016.
- [16] K. Fujimoto and H. Morishita, *Modern Small Antennas*. UK: Cambridge University Press, 2013.
- [17] L. J. Xu, Y. X. Guo, and W. Wu, "Dual-band implantable antenna with open-end slots on ground," *IEEE Antennas Wireless. Propag. Lett.*, vol. 11, pp. 1564–1567, 2012, doi: 10.1109/LAWP.2012.2237010.